

Structural, magnetic, and transport properties of the single-layered perovskites $\text{La}_{2-x}\text{Sr}_x\text{CoO}_4$ ($x=1.0-1.4$)

A. V. Chichev,^{1,2} M. Dlouhá,¹ S. Vratilav,¹ K. Knížek,² J. Hejtmánek,² M. Maryško,² M. Veverka,² Z. Jiráček,² N. O. Golosova,³ D. P. Kozlenko,³ and B. N. Savenko³

¹Faculty of Nuclear Sciences and Physical Engineering CTU Prague, Břehová 7, 115 19 Prague 1, Czech Republic

²Institute of Physics of ASCR, Cukrovarnická 10, 162 53 Prague 6, Czech Republic

³Frank Laboratory of Neutron Physics, Joint Institute for Nuclear Research, 141980 Dubna Moscow Region, Russia

(Received 12 May 2006; revised manuscript received 6 August 2006; published 19 October 2006)

The layered cobaltites $\text{La}_{2-x}\text{Sr}_x\text{CoO}_4$ have been complexly studied over the range of mixed $\text{Co}^{3+/4+}$ valency and their properties discussed in comparison with cubic perovskites $\text{La}_{1-x}\text{Sr}_x\text{CoO}_3$. The sample $x=1.0$ exhibits a paramagnetic ground state based on the intermediate spin state of Co^{3+} and undergoes a broad resistivity transition at 400–900 K, associated with diffusive changes of magnetic susceptibility and volume expansion. The Co^{4+} doping in samples with $x > 1$ induces gradually ferromagnetism and leads to a dramatic decrease of resistivity and thermopower, though the metallicity is not achieved. The neutron diffraction on the limit composition $x=1.4$ suggests that the long-range ordered ferromagnetic regions coexist with paramagnetic ones, and their amount changes little with an application of high pressures up to 4.3 GPa.

DOI: [10.1103/PhysRevB.74.134414](https://doi.org/10.1103/PhysRevB.74.134414)

PACS number(s): 74.25.Ha, 75.30.Wx, 61.12.Ld

I. INTRODUCTION

Transition metal oxides with $3d$ electrons exhibit unusual magnetic and transport properties due to the subtle balance between the crystal-field-splitting Δ_{CF} , the on-site Coulomb repulsion expressed by Hubbard parameter U and the energy of charge transfer between transition metal and oxygen, $\Delta_{\text{TM-O}}$. Particularly interesting are perovskite cobaltites where octahedrally coordinated Co^{3+} ions can exist in three spin states—the nonmagnetic low-spin state that corresponds (in the limit of fully localized electrons in strong crystal field) to filled t_{2g} levels and empty e_g low-spin states (LS, $t_{2g}^6 e_g^0$, $S=0$), and two magnetic states that correspond either to the intermediate spin (IS, $t_{2g}^5 e_g^1$, $S=1$) or to the high-spin states (HS, $t_{2g}^4 e_g^2$, $S=2$). Similarly for Co^{4+} , two spin states are possible, LS ($t_{2g}^5 e_g^0$, $S=0.5$) and IS ($t_{2g}^4 e_g^1$, $S=1.5$) while Co^{2+} ions are reported always as HS ($t_{2g}^5 e_g^2$, $S=1.5$).

The cobaltite system under study belongs structurally to a broader class of Ruddlesden-Popper series $(\text{AO})(\text{ABO}_3)_n$. Ruddlesden-Popper phases are formed by n -layer slabs of perovskite ABO_3 , which are separated by the rock-salt layer AO.¹ For the magnetic and transport properties, it is especially important that the presence of the AO layer disturbs the three-dimensional (3D) periodicity of the perovskite structure. The end members of the Ruddlesden-Popper series, $\text{La}_{2-x}\text{Sr}_x\text{CoO}_4$ ($n=1$, see Fig. 1) and $\text{La}_{1-x}\text{Sr}_x\text{CoO}_3$ ($n=\infty$), represent thus closely related systems with quasi-two-dimensional (2D) and 3D character, respectively.

The $n=\infty$ compounds $\text{La}_{1-x}\text{Sr}_x\text{CoO}_3$ have been studied more extensively than the $n=1$ system $\text{La}_{2-x}\text{Sr}_x\text{CoO}_4$, among other reasons due to its easier preparation, especially for the phases with higher oxidation state of Co. The LaCoO_3 perovskite ($x=0$) is a diamagnetic insulator based on the LS Co^{3+} ground state, and undergoes transition to a paramagnetic state at around 100 K due to thermal population of IS and/or HS excited states.^{2,3} With increasing x , i.e., with the Co^{4+} doping, the ferromagnetic interactions are induced. First, only isolated hole-rich ferromagnetic regions are

formed in the hole-poor diamagnetic matrix at low temperatures. Such systems behave as superparamagnets. The bulk ferromagnetism and metallic conductivity are unambiguously achieved for higher dopings, $x \geq 0.3$.^{4,5}

In the single-layered perovskites $\text{La}_{2-x}\text{Sr}_x\text{CoO}_4$, the valence of Co can be varied over much larger range, hypothetically from Co^{2+} for $x=0$ to Co^{4+} for $x=2$. Extensive data are available for the $\text{Co}^{2+/3+}$ region $x=0-1$. La_2CoO_4 perovskite ($x=0$, Co^{2+}) is an antiferromagnetic insulator with $T_N = 275$ K.^{6,7} The mixed $\text{Co}^{2+/3+}$ valency in the $0 < x < 1$ region brings about magnetic disorder, and spin-glass behavior is found below 100 K for these systems. The electric conduction remains of an activation character. The absolute resistivity steeply decreases with increasing Co^{3+} content. The magnetic and electronic data suggest that Co^{2+} ions are in HS state while Co^{3+} ions gradually change with x from HS to IS state.⁷⁻¹¹

On the other hand, there are less reports concerning the $\text{Co}^{3+/4+}$ region of $\text{La}_{2-x}\text{Sr}_x\text{CoO}_4$ in a composition range up to $x=1.4-1.5$. Similarly to 3D perovskites $\text{La}_{1-x}\text{Sr}_x\text{CoO}_3$, the Co^{4+} doping is associated with the onset of ferromagnetic order that occurs at around 150 K.^{12,13} Early reports on the electrical transport properties concerned the nominal compositions $x=1.0$ and 1.5 only.⁷ For the $x=1.0$ sample the room temperature resistivity $\rho_{300\text{K}} \sim 500$ m Ω cm and the activation energy of $E_A \sim 0.44$ eV are determined, while much lower values $\rho_{300\text{K}} \sim 10$ m Ω cm and $E_A \sim 0.11$ eV are found for $x=1.5$. Very recently, a systematic low-temperature investigation in the range $x=1.0-1.5$ was published by Shimada *et al.*¹⁴ The present work provides an alternative study of the $\text{La}_{2-x}\text{Sr}_x\text{CoO}_4$ system in the region of $\text{Co}^{3+/4+}$ mixed valency by means of the x-ray diffraction, measurements of magnetization, electrical conductivity, and thermoelectric power at low and high temperatures. We exemplify how the quasi-2D character of the samples modifies the low- and high-temperature properties, as compared to their 3D counterparts with a similar extent of hole doping. For a selected composition $x=1.4$, the neutron diffraction experiments at

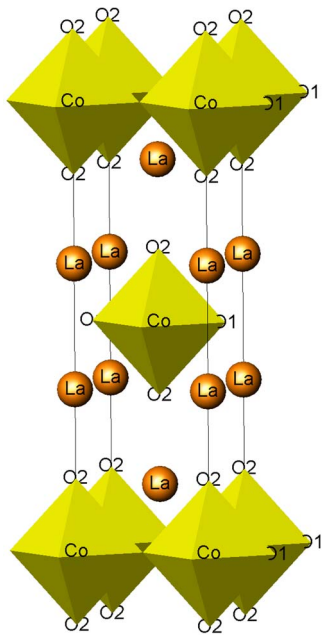


FIG. 1. (Color online) The crystal structure of K_2NiF_2 -type.

ambient pressure and up to 4.3 GPa yields information on the long-range ferromagnetic ordering.

II. EXPERIMENT

The samples $La_{2-x}Sr_xCoO_4$ were prepared for $1.0 \leq x \leq 1.5$. As a first step, fine grain precursors have been made by a sol-gel method. The corresponding amounts of La_2O_3 , $SrCO_3$, and $Co(NO_3)_2$ were separately dissolved in nitric acid. The solute was mixed with citric acid and ethylene glycol in the ratio of $(2-x[La]+x[Sr]+[Co])/1.5$ [citric acid]/ 2.25 [ethylene glycol] and pH factor was adjusted to 9 by the addition of NH_4OH . In the next step, the gel was made by the evaporation of water at $80-90^\circ C$. After drying at $160^\circ C$ and calcination at $400^\circ C$ (4 h in air), the resulting powder was ground, pressed into pellets, and sintered at $1000^\circ C$ for 100 h in an oxygen atmosphere. The x-ray diffraction analysis (Bruker D8, $CuK\alpha$, SOL-X energy dispersive detector) detected the single $n=1$ Ruddlesden-Popper phase up to $x=1.4$. In the case of $x=1.5$, traces of unknown impurity were observed. Consequently, more detailed investigation of physical properties was performed up to the limit $x=1.4$. Simultaneous measurements of the electrical resistivity and thermoelectric power between $10-1000$ K were performed in a close cycle refrigerator (up to 300 K) or using a small tubular furnace with precisely controlled temperatures. The standard E-type (K-type) thermocouples were used for the monitoring of a temperature gradient, imposed across the sample by means of an additional heater. In both cases the four-point steady state methods for the electrical resistivity were applied.

The low-temperature magnetic measurements were done using the SQUID magnetometer. Magnetization curves were measured in fields up to 5 T, the DC susceptibility was measured at fields of 0.01, 0.1, and 1 T. The measurements

on samples $x=1.0$ and 1.1 revealed some ferromagnetic (La,Sr) CoO_3 impurity ($T_C=250$ K). Its molar concentration in the studied materials was estimated to be about 0.3% in maximum. Despite of such very low value, the parasitic ferromagnetism could influence the measurements at 0.01 T, and higher fields were applied in order to saturate the impurity magnetization and to allow a separation of intrinsic paramagnetic susceptibility in samples $x=1.0$ and 1.1 below 250 K. Alternative data on the low-temperature paramagnetic susceptibility, practically insensitive to the impurity, were obtained by differential measurements at two close fields 1 and 1.25 T. Finally, the high-temperature susceptibility of $La_{2-x}Sr_xCoO_4$ (up to 800 K) was measured at a field of 1 T using a compensated pendulum system, MANICS.

Lattice parameters and atomic coordinates within the $I4/mmm$ space group symmetry were determined at room temperature by x-ray powder analyses using the FULLPROF program. The neutron diffraction has been performed on a selected sample $x=1.4$ on the diffractometer KSN-2 at room temperature using an improved resolution and neutron wavelength $\lambda=1.363$ Å. The study was completed down to low temperatures, both at normal pressure and up to 4.3 GPa, on the high pressure diffractometer DN-12 at pulsed reactor IBR-2. The time-of-flight spectra were taken using two detector banks situated at scattering angles $2\vartheta=45.5^\circ$ and 90° , covering a broad range of interplanar spacings $d=1-10$ Å. The experimental data were analyzed with the Rietveld method using the MRJA and FULLPROF programs.

III. RESULTS

A. Structural parameters

The crystal symmetry of $La_{2-x}Sr_xCoO_4$ is tetragonal (space group $I4/mmm$). Cobalt ions are coordinated by an elongated oxygen octahedron with four O1 ligands in the equatorial plane and two more displaced O2 ligands in the apical direction along the c axis. La, Sr ions are in a nine fold coordination with four oxygen O2 sites in the equatorial plane, one O2 site in the apical position, and four O1 sites directed to the opposite demisphere (see Fig. 1). Lattice parameters observed at room temperature are shown in Fig. 2. The calculated bond lengths are displayed in Fig. 3.

The unit cell volume is monotonously decreasing over the range $x=1.0-1.5$. The evolution of lattice parameters is more complex. There is a rapid contraction of parameter a up to $x=1.2$, which is partially compensated by an enhancement of parameter c . For higher x the parameter a saturates almost at a constant value, while c reaches a local maximum and then decreases. Similar lattice parameters of $La_{2-x}Sr_xCoO_4$ are reported in.¹⁴ In earlier reports,^{12,15} a similar trend of lattice parameters is observed but there is a distinct shift in the absolute values that may be associated with differences in sample preparation.

For the understanding of the complex lattice evolution with x , two individual contributions have to be considered: (i) the Co ionic radius is reduced due to oxidation $Co^{3+} \rightarrow Co^{4+}$, (ii) at the same time La^{3+} ($r(La^{3+})=1.216$ Å) is being replaced by larger Sr^{2+} [$r(Sr^{2+})=1.31$ Å]. This latter effect is demonstrated in Fig. 3 by an increase of the average

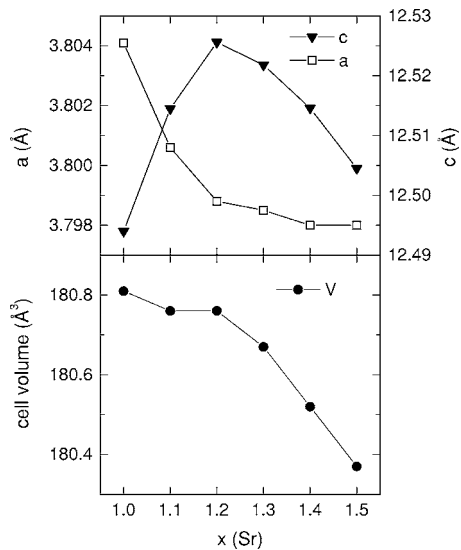


FIG. 2. The lattice constants and the unit cell volume for $\text{La}_{2-x}\text{Sr}_x\text{CoO}_4$.

La/Sr-O bond with x in a rate which is in good agreement with the above-mentioned La, Sr radii. The evolution of Co-O1 equatorial distance and La/Sr-O2 equatorial distance is identical with that of a parameter. Observed shortening of these bond lengths for $x \leq 1.2$ can be attributed to the reduction of $\text{Co}^{3+/4+}$ ionic radius, considering that the (La, Sr)O planes in the $\text{La}_{2-x}\text{Sr}_x\text{CoO}_4$ structure for $x \sim 1$ are in a tensile stress while the CoO_2 perovskite plane is under compressive stress. The reduction of $\text{Co}^{3+/4+}$ size acts thus primarily on the equatorial Co-O1 distances. The decrease is saturated at higher x due to competition with the enlarging size of the La, Sr-site. Then, the Co-O2(apical) distance starts to decrease more steeply. In the case of La/Sr-O1 bond, the influence of

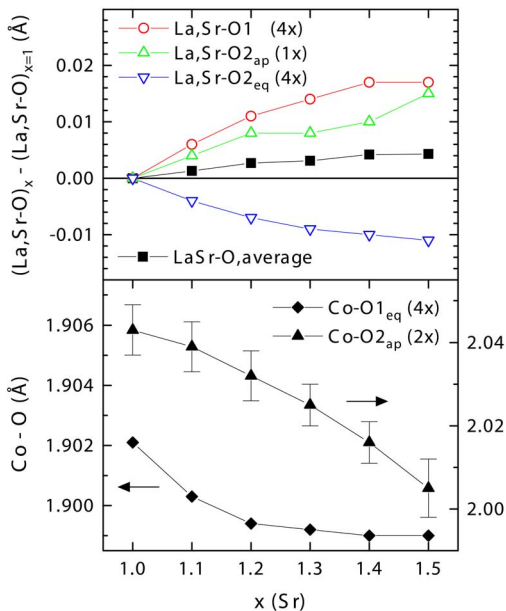


FIG. 3. (Color online) Lower panel: Co-O bond lengths in $\text{La}_{2-x}\text{Sr}_x\text{CoO}_4$. Upper panel: The change of the (La, Sr)-O bond length relative to the $x=1$ sample.

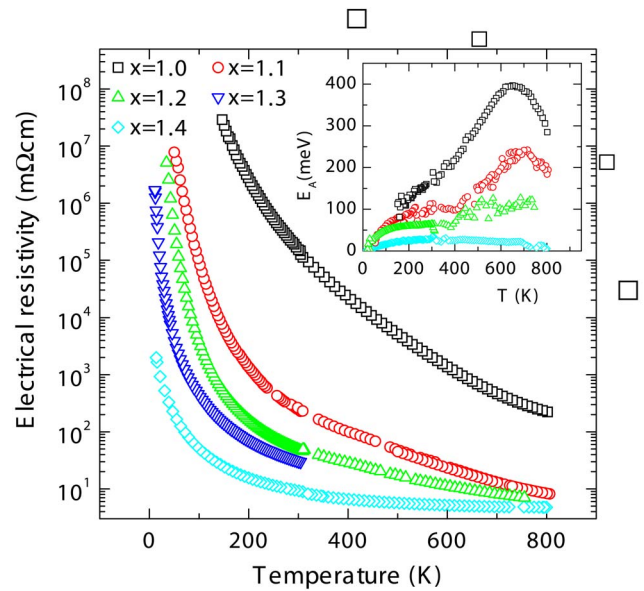


FIG. 4. (Color online) The electrical resistivity and local activation energy defined as $E_A = d(\ln\rho)/d(1/T)$ for $\text{La}_{2-x}\text{Sr}_x\text{CoO}_4$.

competing Co-O1(equatorial) is smaller so the bond increases rather quickly up to $x=1.4$. As concerns the apical bonds forming Co-O2-La/Sr-O2-La/Sr-O2-Co... chains along the c axis, the stacking of perovskite and rock-salt layers does not pose any structural constraints and the effect of the La, Sr-site expansion is straightforward, leading to a steady increase of La/Sr-O2 apical distance.

B. Electrical resistivity and thermopower

The electrical resistivity data measured up to 900 K are shown in Fig. 4. The displayed curves evidence for all samples an activation character of the electric transport that persists in the whole temperature range. Even if the temperature dependence seems to be monotonous, the calculation of local activation energy defined as $E_A = d(\ln\rho)/d(1/T)$ (see inset of Fig. 4) shows for the nominally single valent (Co^{3+}) sample $x=1.0$ a broad peak centered at around 650 K. This is a clear signature of diffusive electronic transition originating from the electron and/or hole excitations in this essentially nonconducting sample. A similar but much narrower transition was observed in LaCoO_3 at 535 K.¹⁶ When holes are introduced by increased strontium doping in $\text{La}_{2-x}\text{Sr}_x\text{CoO}_4$ ($x > 1$), the room-temperature electrical resistivity decreases significantly (simultaneously with a drop of activation energy) down to a quasimetallic value ~ 10 mΩ cm for $x=1.4$. (This absolute value is about one order of magnitude lower than reported for the same composition in Ref. 14; the low-temperature localization is otherwise similar.)

The thermopower data, displayed in Fig. 5, are coherent with the resistivity changes. All the samples $x=1.0-1.4$ show the temperature dependence of an activation type. Nonetheless, a thermodynamical turn down towards zero at low temperatures points to the absence of the energy gap; in other words, there is a final density of states at Fermi level, persisting down to the lowest temperatures. The maximum

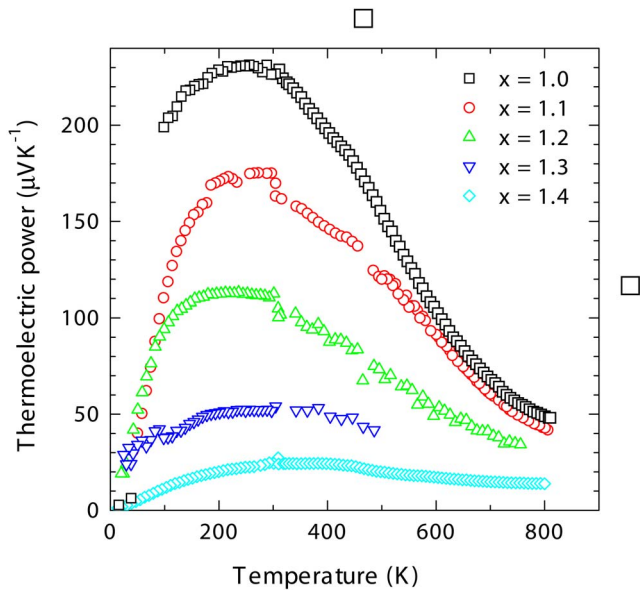


FIG. 5. (Color online) The thermoelectric power in $\text{La}_{2-x}\text{Sr}_x\text{CoO}_4$.

thermopower coefficient is reached at around room temperature, independently on x , and its absolute values decrease rapidly with x . This points to an increasing number of mobile carriers in the $\text{La}_{2-x}\text{Sr}_x\text{CoO}_4$ system for $x > 1.0$.

C. Magnetic measurements

Earlier studies on the $\text{Co}^{2+}/\text{Co}^{3+}$ single crystals $\text{La}_{2-x}\text{Sr}_x\text{CoO}_4$ suggest that the pure Co^{3+} compound $x=1.0$ is paramagnetic down to the lowest temperatures.⁸ As mentioned in the experimental part, the low-temperature susceptibility data measured in low field of 0.01 T are very sensitive to any ferromagnetic impurity. This leads to spurious effects seen especially in the plot of inverse susceptibility as presented, e.g., in Fig. 5 of Shimada *et al.* in Ref. 14. The authors related their observation to the theoretical conception of Griffith phase where a system with ferromagnetic interactions of random strength displays critical fluctuations in a broad temperature range between the maximum “local” critical temperature (close to T_C of bulk ferromagnet Sr_2CoO_4) and much lower global T_C .¹⁷ We remain with the more prosaic explanation considering the cubic perovskite $\text{La}_{1-x}\text{Sr}_x\text{CoO}_3$ impurity ($T_C=200$ and 250 K for $x=0.2$ and 0.5, respectively¹⁸) and refer to the measurements at $H=1$ T on our ceramic sample in the upper panel of Fig. 6. Here, the impurity ferromagnetic contribution is easily separated and, after the correction, the susceptibility acquires a Curie-type dependence close to what is expected for paramagnetic IS Co^{3+} ions ($S=1$). The molar fraction of the impurity is determined to about 0.3%. We observed, however, that the amount of ferromagnetic impurity is dependent on sample preparation, in particular it increases with increasing temperature of synthesis. In these samples the $\text{La}_{1-x}\text{Sr}_x\text{CoO}_3$ impurity could reach several % and have been then identified by the x-ray diffraction.

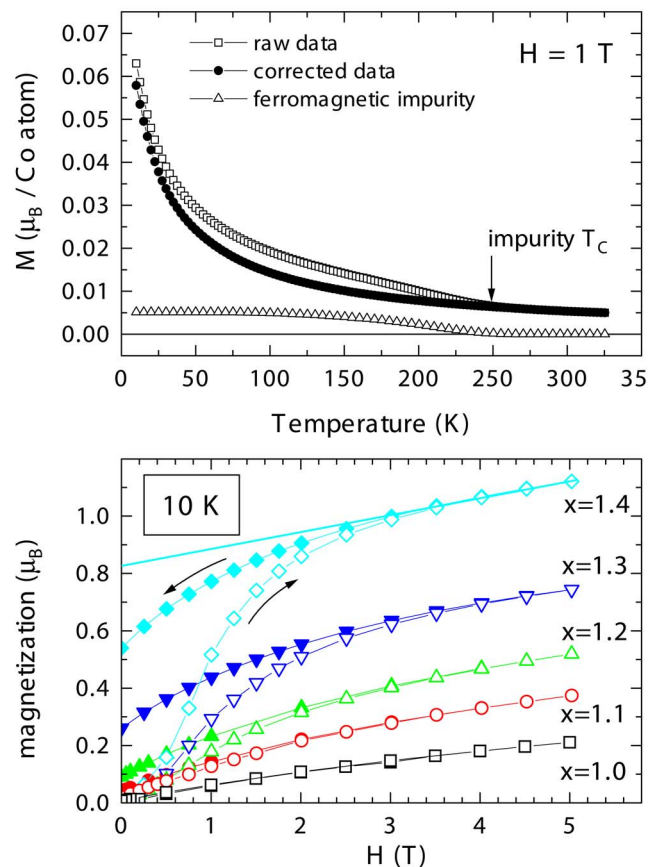


FIG. 6. (Color online) Upper panel: Magnetization for LaSrCoO_4 ($x=1.0$), measured on cooling in 1 T. (\square) Raw data; (\bullet) data after correction; (\triangle) ferromagnetic impurity. Lower panel: Magnetization loops for $\text{La}_{2-x}\text{Sr}_x\text{CoO}_4$ at 10 K.

For samples $x=1.1$ and less reliably for $x=1.2$, a similar correction reveals a still smaller impurity fraction, which is another argument against the explanation using the Griffith phase.

For $\text{Co}^{3+}/\text{Co}^{4+}$ samples with $x=1.1-1.4$, the magnetization curves at 10 K, presented in the lower panel of Fig. 6, reveal a formation of ferromagnetic regions. Saturation moments, obtained by the linear extrapolation, increase rapidly with Co^{4+} doping and reach $0.8\mu_B/\text{Co}$ atom for $x=1.4$. This value is about twice lower than expected for a bulk ferromagnetic state with a mixture of IS Co^{3+} ($S=1$) and LS Co^{4+} ($S=0.5$) ions, which are the spin states adopted for cubic ferromagnetic perovskites $\text{La}_{1-x}\text{Sr}_x\text{CoO}_3$ (see, e.g., Ref. 19). The observed saturation moments and large paraprocess even at the lowest temperatures suggest a more complex, possibly nonuniform magnetic ground state in the present ferromagnetic samples, which led us actually to a more detailed investigation of the $x=1.4$ compound by neutron diffraction (see below).

The plot of inverse susceptibility versus temperature in a range up to 800 K is presented in the upper panel of Fig. 7. Here, the diamagnetic signal of core electrons in $\text{La}_{2-x}\text{Sr}_x\text{CoO}_4$, estimated as $\chi_{\text{dia}}=-1.02 \times 10^{-4}$ emu/mol,²⁰ was subtracted from experimental data (effect is significant at high temperatures only) while the low-temperature suscep-

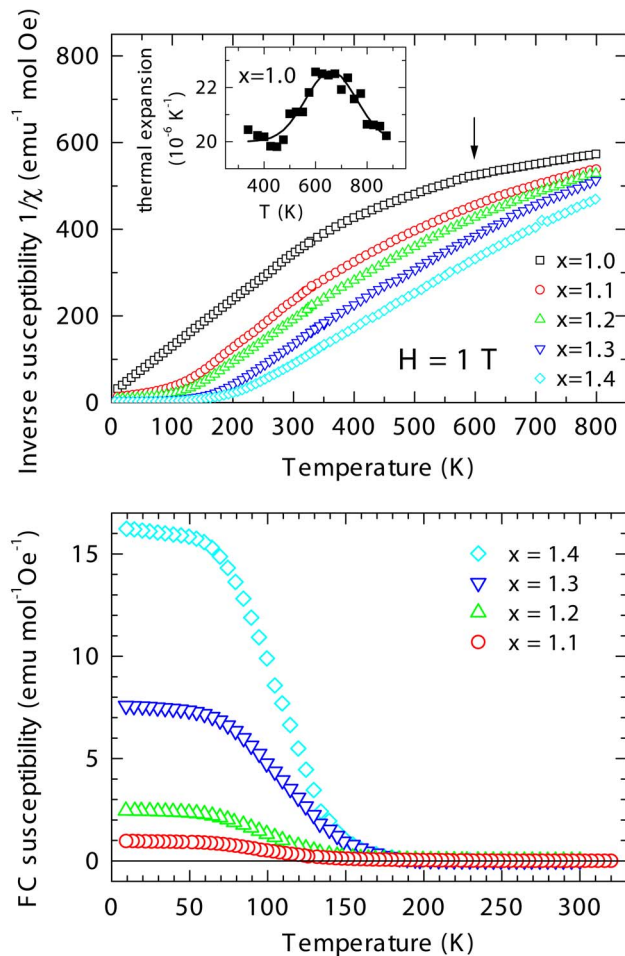


FIG. 7. (Color online) The temperature dependence of the magnetic susceptibility for $\text{La}_{2-x}\text{Sr}_x\text{CoO}_4$ ($1.0 \leq x \leq 1.4$). Lower panel: FC DC susceptibility in 0.01 T. Upper panel: inverse DC susceptibility in field of 1 T (small change of slope associated with the resistivity transition in $x=1.0$ is marked by arrow). Inset: averaged linear coefficient of lattice thermal expansion for $x=1.0$. Solid line is Gaussian fit, see Ref. 16 for details.

tibility data were corrected for the ferromagnetic (La,Sr)CoO₃ impurity. It should be noted that differential susceptibility, evaluated on a base of magnetization measurements at two close fields, 1 and 1.25 T, yielded practically the same data as the DC susceptibilities after subtraction of the ferromagnetic impurity contribution.

The simple Curie-Weiss behavior of the low-temperature inverse susceptibility for sample LaSrCoO_4 ($x=1.0$) is fitted by a slightly negative Weiss temperature $\Theta = -20$ K and the effective moment of $\mu_{\text{eff}} \sim 2.7\mu_B$. At elevated temperatures, the inverse susceptibility deviates progressively from the linear dependence and, in addition, some more abrupt change of slope can be distinguished at about 600 K. This anomaly is obviously associated with the resistivity transition in this sample (see the apparent activation energy in the inset of Fig. 4). In cubic perovskite LaCoO_3 , the analogous resistivity transition centered at 535 K is accompanied by a spin-state transition of Co^{3+} ions, characterized by a change of effective moment from $\mu_{\text{eff}} \sim 3.2\mu_B$ ($T=150-350$ K) to μ_{eff}

$= 3.84\mu_B$ for $T > 650$ K (see, i.e., Fig. 6 in Ref. 21). Similar spin-state transitions can be anticipated in present layered compounds with $x \geq 1.0$. However, they are more diffusive and not completed below 800 K, the limit of our magnetic data determination.

Magnetic transitions in cobaltites are also accompanied by subtle changes in the crystal structure, induced by expanding ionic radius of Co^{3+} with a change of spin state. This effect is responsible for an anomalous thermal expansion that reflects the increasing population of paramagnetic species. An anomalous peak in the linear thermal expansion coefficient is also observed in our sample LaSrCoO_4 at 660 K by x-ray diffraction, see the inset of Fig. 7. The data show that the normal lattice expansion out of the peak is around $20 \times 10^{-6} \text{ K}^{-1}$ as in LnCoO_3 ($\text{Ln}=\text{La}, \text{Y}, \text{rare-earth}$) while the peak characterizing the transition is more diffusive and the integral volume change is only 0.25%, that is about four times less than observed for LnCoO_3 .¹⁶ The smaller volume change during the transition may have two reasons. In a distinction to the close-packed structure of LnCoO_3 , where any change of Co-O bond distance or angle produces a corresponding change of lattice parameters, in the LaSrCoO_4 structure the expansion of CoO_6 octahedra in the c direction can be partially compensated by a decrease of (La, Sr)-O bond distances. However, the low sensitivity of x-ray diffraction to oxygen did not allow us to determine the expansion of CoO_6 octahedra itself. The second reason may be a different character of spin states in LnCoO_3 and LaSrCoO_4 below or above the magnetic transition.

With the Co^{4+} doping, the ferromagnetic interactions are clearly induced as seen already for $x=1.1$, and the extrapolated Weiss temperature increases steadily up to $\Theta=190$ K for $x=1.4$. However, the ferromagnetic transition itself seems to shift down to much lower temperatures. This becomes evident in the plot of susceptibility measured at a low magnetic field of 0.01 T (see the lower panel of Fig. 7). It appears that at some critical temperature $T_C=140-150$ K, the susceptibility for $x=1.3$ and 1.4 starts to increase enormously and finally levels at ~ 70 K. This is a signature for a gradual change from a short range or two-dimensional (2D) ferromagnetic order in the perovskite layers to a stabilization of the (3D) ordered ferromagnetic regions below 70 K. Their amount increases quickly with x .

The values of Θ and μ_{eff} for $\text{La}_{2-x}\text{Sr}_x\text{CoO}_4$, derived from linear regions of inverse susceptibility in Fig. 7 and completed by previous data for $x=0.4-1.0$,⁸ are summarized in Fig. 8. Weiss temperature increases nearly monotonously from $\Theta=-200$ K for $x=0.4$ up to $\Theta=190$ K for $x=1.4$, and is symmetrically centered around $x=1.0$ where the change from antiferromagnetic interactions to ferromagnetic ones occurs. The effective moment decreases from $\mu_{\text{eff}} \sim 4\mu_B$ for the $\text{Co}^{2+}/\text{Co}^{3+}$ sample $x \sim 0.5$ to $\mu_{\text{eff}} \sim 2.7\mu_B$ for pure Co^{3+} sample $x=1.0$. This is essentially in accordance with expected spin states for HS Co^{2+} ($S \sim 1.5$, $\mu_{\text{eff}} \sim 3.87\mu_B$) and IS Co^{3+} ($S \sim 1$, $\mu_{\text{eff}} \sim 2.83\mu_B$). For Co^{4+} -doped samples with $x > 1.0$, the effective moment first levels at $\mu_{\text{eff}} \sim 2.7-2.8\mu_B$ but finally increases to $\mu_{\text{eff}}=3.1\mu_B$ for $x=1.4$, pointing to a stabilization of IS Co^{4+} state.

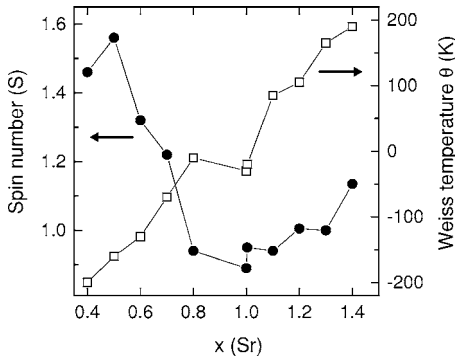


FIG. 8. The composition dependence of Weiss temperature Θ data and effective spin number S [$\mu_{\text{eff}}=2\sqrt{S(S+1)}$], derived from linear regions of inverse susceptibility for $\text{La}_{2-x}\text{Sr}_x\text{CoO}_4$ in Fig. 7. (Data for $0.4 < x < 1.0$ are taken from Ref. 8.)

D. Neutron diffraction on sample $x=1.4$ up to high pressures

The powder diffraction patterns of $\text{La}_{0.6}\text{Sr}_{1.4}\text{CoO}_4$ taken on constant wavelength diffractometer KSN-2 (at $P=0$ GPa, $T=300$ K) and time-of-flight diffractometer DN-12 (at $P=0$ and 4.3 GPa, $T=290, 16$, and 10 K) is shown in Figs. 9 and 10, respectively. At ambient pressure, the low-temperature spectra ($T=16$ K) do not show any new diffraction line that could be ascribed to an antiferromagnetic order. On the other hand, existence of a long-range ferromagnetic order is evidenced by an intensity contribution to some fundamental diffraction lines. This is illustrated in more detail in the inset of Fig. 10 where observed intensity at line (103) exceeds significantly the calculated intensity for nuclear scattering while no additional intensity is observed at line (004). This observation determines that the spontaneously ordered cobalt moments are oriented along the c axis of the $I4/mmm$ structure, i.e., perpendicular to the layers. Their calculated magnitudes amount to $0.7\mu_B/\text{Co}$ atom, which is in agreement with the magnetization data in the lower panel of Fig. 6.

A low value of spontaneous moments suggests that the ferromagnetic transition remains incomplete, leading to a ferromagnetic-paramagnetic segregation. Since the magnetic interactions are associated with electron transfer, either real (double exchange) or virtual (superexchange), they are extremely sensitive to the transition metal $3d$ -oxygen $2p$ orbital overlap. It appears that the overlap integrals and, conse-

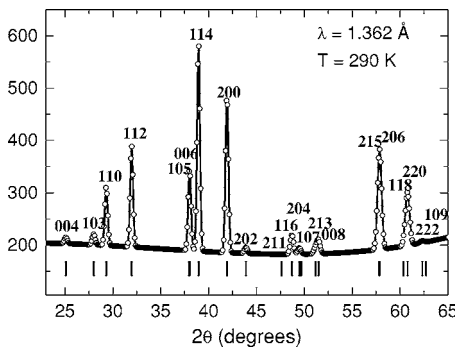


FIG. 9. The neutron diffraction pattern of $\text{La}_{0.6}\text{Sr}_{1.4}\text{CoO}_4$ measured on the KSN-2 diffractometer at $T=290$ K.

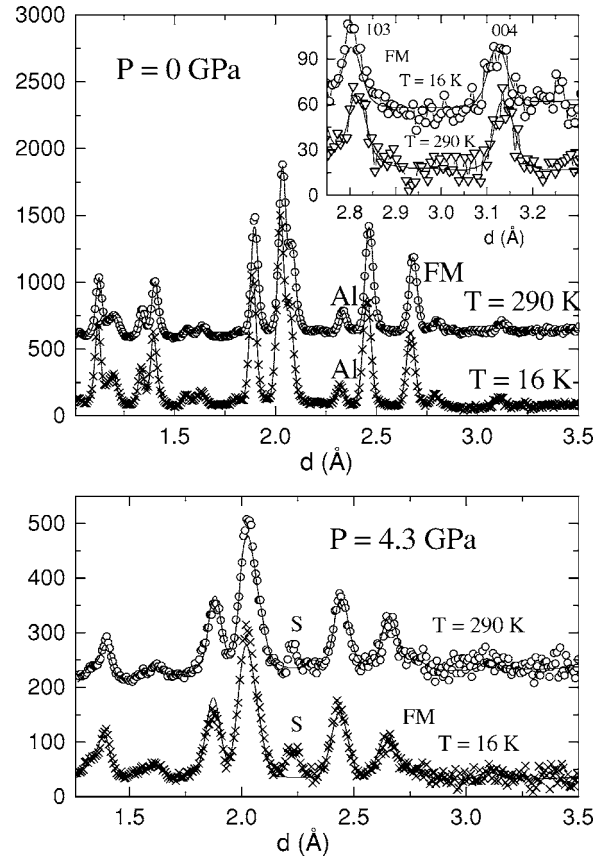


FIG. 10. The neutron diffraction patterns of $\text{La}_{0.6}\text{Sr}_{1.4}\text{CoO}_4$ measured at $T=290$ and 16 K at ambient pressure (upper panel) and 4.3 GPa (lower panel). The experimental points and calculated profile are shown. The position of the most intense peak from Al container used at ambient pressure is also shown. The position of the diffraction peak from the high pressure cell is marked by “S.”

quently, the double exchange vary with the metal-oxygen bond lengths approximately according to a power dependence $\sim l^{-3.5}$ while the superexchange may vary even much more steeply.²² Therefore, one would expect enhancement of the magnetic interactions on lattice contraction, forced by high pressures. The possibility to induce more ferromagnetic phase was a primary motivation for a high-pressure neutron-diffraction study of $\text{La}_{0.6}\text{Sr}_{1.4}\text{CoO}_4$. The analysis of observed spectra showed, however, only a modest increase of ferromagnetically ordered cobalt moments from $0.7\mu_B$ at ambient pressure to $0.9\mu_B$ at 4.3 GPa.

Complete results obtained by the neutron-diffraction studies of $\text{La}_{0.6}\text{Sr}_{1.4}\text{CoO}_4$ are summarized in Table I. The room-temperature data at different pressures allow us to calculate linear compressibilities $k_i = -(1/a_{i0})(da_i/dP)_T$ both for the lattice parameters ($k_a=0.0011$ GPa⁻¹, $k_c=0.0007$ GPa⁻¹) and the equatorial and apical Co-O bond lengths ($k_{\text{Co-O1}}=0.0011$ GPa⁻¹, $k_{\text{Co-O2}}=0.004(1)$ GPa⁻¹). Similar values are observed at low temperatures, $k_a=0.0011$ GPa⁻¹, $k_c=0.0006$ GPa⁻¹, $k_{\text{Co-O1}}=0.0011$ GPa⁻¹, $k_{\text{Co-O2}}=0.003(1)$ GPa⁻¹. This shows that the lattice compressibility is lower along c , i.e., between the perovskite layers. Despite this, there is an unexpectedly high compressibility of the Co-O2 (apical) bond, which is compensated by expansion under an

TABLE I. Structural parameters of $\text{La}_{0.6}\text{Sr}_{1.4}\text{CoO}_4$ at selected pressures and ambient temperature. The atomic positions are La/Sr and O2-4(*e*) (0, 0, *z*), Co-2(*a*) (0, 0, 0) and O1-4(*c*) (0.5, 0, 0) of the space group $I4/mmm$. Values of Co-O1 and Co-O2 bond lengths and the Co magnetic moments are also presented. (Data from KSN-2 are added in the first column.)

<i>P</i> , (GPa)	0 (KSN-2)	0	0	2	2	4.3	4.3
<i>T</i> , K	290	290	16	290	12	290	10
<i>a</i> , Å	3.7983(3)	3.798(4)	3.790(4)	3.778(5)	3.770(5)	3.768(5)	3.756(5)
<i>c</i> , Å	12.514(8)	12.516(7)	12.488(7)	12.476(9)	12.461(9)	12.441(9)	12.425(9)
La/Sr (<i>z</i>)	0.3589(4)	0.3585(6)	0.3586(6)	0.358(2)	0.358(2)	0.361(2)	0.358(2)
O2 (<i>z</i>)	0.1604(4)	0.1606(7)	0.1593(7)	0.155(3)	0.157(3)	0.155(3)	0.156(3)
Co-O1, Å (4 <i>x</i>)	1.899(1)	1.899(2)	1.895(2)	1.889(3)	1.885(3)	1.884(3)	1.878(3)
Co-O2, Å (2 <i>x</i>)	2.007(5)	2.010(4)	1.989(4)	1.93(1)	1.95(1)	1.93(1)	1.94(1)
La/Sr-O1, Å (4 <i>x</i>)	2.593(7)	2.597(6)	2.590(6)	2.59(1)	2.59(1)	2.56(1)	2.58(1)
La/Sr-O2, Å (4 <i>x</i>)	2.686(2)	2.686(3)	2.680(3)	2.671(4)	2.666(4)	2.664(4)	2.656(4)
La/Sr-O2, Å (1 <i>x</i>)	2.484(9)	2.477(8)	2.489(8)	2.53(2)	2.51(2)	2.56(2)	2.51(2)
μ , μ_B			0.7(1)		0.8(1)		0.9(1)
R_p , %	2.58	6.63	4.27	7.16	10.10	7.84	8.29
R_{wp} , %	2.44	4.34	3.13	6.34	8.11	7.80	7.96

external field of the shortest La/Sr-O2 (apical) bond length. This seemingly anomalous effect can be attributed to the opposite stresses in the CoO_2 and (La, Sr)O layers as mentioned with the x-ray diffraction results.

IV. DISCUSSION

It is generally accepted that the magnetism and transport in mixed valent perovskites are predetermined by the extent of carrier doping, bandwidth (linked to the metal-oxygen overlap), and local disorder due to substitutional defects. Lowering of the dimensionality in the layered $\text{Co}^{3+}/\text{Co}^{4+}$ systems $\text{La}_{2-x}\text{Sr}_x\text{CoO}_4$, compared to their 3D counterparts, brings about an anisotropic reduction of the bandwidth, which modifies physical properties. As concerns the pure Co^{3+} compound $x=1.0$ (LaSrCoO_4), the high values of thermopower coefficients and electrical resistivity are signatures of the absence of mobile charge carriers. This is consistent, together with observed $\mu_{\text{eff}} \sim 2.7\mu_B$, with an insulating paramagnetic ground state. It is based on IS Co^{3+} ions that are in orbitally nondegenerate state ($d_{yz}^2 d_{zx}^2 d_{xy}^1 d_{z^2}^1$, $S=1$) as one may expect for tetragonally elongated CoO_6 octahedra in layered perovskites (see also Ref. 23). On the other hand, isovalent 3D counterpart LaCoO_3 is a diamagnetic insulator and the paramagnetic state with strong antiferromagnetic interactions and low electrical conductivity, occurring above 100 K, is most likely based on a mixture of LS and HS Co^{3+} rather than on a homogeneous IS state. (For the latter eventuality, a formation of a partially occupied σ^* band and metallicity could be anticipated in 3D perovskites; see, e.g., the recent discussion in Ref. 24.)

The Co^{4+} doping in samples with $x > 1.0$ leads to a rapid decrease of resistivity and thermoelectric power due to the presence of mobile carriers. The metallic conductivity is common for analogous 3D systems both in low-temperature ferromagnetic and high-temperature paramagnetic states. In

particular, $\text{La}_{1-x}\text{Sr}_x\text{CoO}_3$ exhibits for $x=0.3-0.5$ very low resistivity $\rho_{300\text{ K}} \leq 1\text{ m}\Omega\text{ cm}$ and thermopower $S_{300\text{ K}} \sim 0\text{ }\mu\text{V/K}$ ($T_C=250\text{ K}$). Such a situation is not achieved for the present layered compound $x=1.4$ ($E_A \sim 0.03\text{ meV}$, $\rho_{300\text{ K}}=10\text{ m}\Omega\text{ cm}$ and $S_{300\text{ K}} \sim 30\text{ }\mu\text{V/K}$). It should be mentioned, however, that the absolute resistivity values can be strongly affected by low grain connectivity in our ceramic samples as the sintering was done at a low temperature $\sim 1000\text{ }^\circ\text{C}$. Activation itself is likely an intrinsic effect and, combined with the significant but nonactivated thermoelectric power at low temperatures, points to the polaronic character of itinerant charge carriers in Co^{4+} -doped $\text{La}_{2-x}\text{Sr}_x\text{CoO}_4$.

At low temperatures, ferromagnetism is gradually formed in the doped $\text{La}_{2-x}\text{Sr}_x\text{CoO}_4$. Up to $x=1.2$, only a partial, presumably two-dimensional order is observed. With further increase of the strontium amount, a gradual transition to the 3D ferromagnetic order starts below 150 K and is saturated at about 70 K. The amount of the long-range ordered ferromagnetic phase increases with x and, as found by magnetization measurements and neutron diffraction, the saturation moment reaches for $x=1.4$, a value of $0.7-0.8\mu_B/\text{Co}$ atom and does not change much under an application of external pressure of several GPa. This points to an approximate phase separation where ferromagnetic regions coexist with residual paramagnetic or 2D-ordered regions. Local critical temperatures ($T_C=150\text{ K}$ in maximum) and ordered moments are low compared to what is observed by the neutron diffraction on cubic perovskite $\text{La}_{1-x}\text{Ba}_x\text{CoO}_3$ with $x=0.5$ ¹⁶ or in magnetization measurements of $\text{La}_{1-x}\text{Sr}_x\text{CoO}_3$ systems with $x=0.3-0.5$ ($T_C \sim 250\text{ K}$, saturation moment $1.9\mu_B/\text{Co}$ atom). The low values observed for the present system need not be related to the lower dimensionality only, since there can be also an effect of local disorder. Namely, the magnetic and neutron diffraction studies on ferromagnetic $\text{SrCoO}_{3-\delta}$ ²⁵ showed a systematic decrease of critical temperature and saturation moment with increasing oxygen deficiency from

the nearly 100% Co^{4+} sample with $\delta=0.03$ ($T_C \sim 191$ K, $1.5\mu_B/\text{Co}$ atom) to the 40% Co^{4+} sample with $\delta=0.30$ ($T_C \sim 150$ K, $0.6\mu_B/\text{Co}$ atom) which is analogous to the present $x=1.4$ as to the cobalt valency.

It is worth mentioning that in agreement with our results on $x=1.4$ nearly identical moment and critical temperature, as well as similar transport behavior were obtained for related layered system $\text{Y}_{2-x}\text{Sr}_x\text{CoO}_4$ for $x=1.5$ ($0.75\mu_B/\text{Co}$ atom, $T_C=150$ K, activation energy at around the room-temperature $E_A \sim 0.05$ meV).²³ The pure Co^{4+} compound Sr_2CoO_4 ($x=2.0$), prepared under high pressures, then possessed a significantly larger saturation moment $1.0\mu_B/\text{Co}$ atom and $T_C=250$ K, and showed in the paramagnetic region relatively high conductivity with very small activation energy $E_A \sim 0.01$ meV.

V. CONCLUSION

The layered perovskites $\text{La}_{2-x}\text{Sr}_x\text{CoO}_4$ have been studied in a compositional range from $x=1.0$ (pure Co^{3+}) to $x=1.4$ (40% of Co^{4+}). The evolution of the crystal in dependence on x and on the application of high pressures up to 4.3 GPa (for $x=1.4$ only) is explained by the effect of opposite stresses in the perovskite CoO_2 and rock-salt (La, Sr)O planes.

All samples exhibit an activated type of electrical conduction, however, the absolute values of electrical resistivity and associated activation energy decrease dramatically with x .

Even if the metallic conductivity is not achieved, the gapless character of thermopower is an argument for ground state with itinerant polaronic carriers in the Co^{4+} -doped $\text{La}_{2-x}\text{Sr}_x\text{CoO}_4$.

Magnetic properties demonstrate aparamagnetic ground state with intermediate-spin Co^{3+} ions in the single valent $x=1.0$, which is in distinction with the diamagnetic ground state in analogous cubic perovskite LaCoO_3 . In samples $\text{La}_{2-x}\text{Sr}_x\text{CoO}_4$ with higher strontium content, the itinerant carriers mediate ferromagnetic interactions that give rise to a short range or a two-dimensional FM order that is transformed for higher x to a 3D ferromagnetism.

At elevated temperatures, the magnetic susceptibility $\text{La}_{2-x}\text{Sr}_x\text{CoO}_4$ deviates from the common Curie-Weiss behavior. This is ascribed to a gradual change of the $\text{Co}^{3+/4+}$ spin states. In samples $x=1.0$ and 1.1, there is, in addition, a broad resistivity transition centered at 650 K, which is accompanied by an anomalous lattice expansion. This observation reminds us of the “insulator-metal” transition in LaCoO_3 at 535 K.

ACKNOWLEDGMENT

This work was done as a part of the Project No. 202/06/0051 of the Grant Agency of the Czech Republic. Neutron diffraction experiments were supported by the Project No. A100100611 of the Grant Agency of the ASCR and Project of JINR No. 7-4-1031-99/08.

-
- ¹S. N. Ruddlesden and P. Popper, *Acta Crystallogr.* **10**, 538 (1957).
- ²M. A. Señarís-Rodríguez and J. B. Goodenough, *J. Solid State Chem.* **118**, 323 (1995).
- ³K. Asai, O. Yokokura, M. Suzuki, T. Naka, T. Matsumoto, H. Takahashi, N. Mori, and K. Kohn, *J. Phys. Soc. Jpn.* **66**, 967 (1997).
- ⁴R. Caciuffo, D. Rinaldi, G. Barucca, J. Mira, J. Rivas, M. A. Señarís-Rodríguez, P. G. Radaelli, D. Fiorani, and J. B. Goodenough, *Phys. Rev. B* **59**, 1068 (1999).
- ⁵R. Caciuffo, J. Mira, J. Rivas, M. A. Señarís-Rodríguez, P. G. Radaelli, F. Carsughi, D. Fiorani, and J. B. Goodenough, *Europhys. Lett.* **45**, 399 (1999).
- ⁶K. Yamada, M. Matsuda, Y. Endoh, B. Keimer, R. J. Birgeneau, S. Onodera, J. Mizusaki, T. Matsuura, and G. Shirane, *Phys. Rev. B* **39**, 2336 (1989).
- ⁷T. Matsuura, J. Tabuchi, N. Mizusaki, S. Yamauchi, and K. Fueki, *J. Phys. Chem. Solids* **49**, 1403 (1988); **49**, 1409 (1988).
- ⁸Y. Moritomo, K. Higashi, K. Matsuda, and A. Nakamura, *Phys. Rev. B* **55**, R14725 (1997).
- ⁹I. A. Zaliznyak, J. M. Tranquada, R. Erwin, and Y. Moritomo, *Phys. Rev. B* **64**, 195117 (2001).
- ¹⁰I. A. Zaliznyak, J. P. Hill, J. M. Tranquada, R. Erwin, and Y. Moritomo, *Phys. Rev. Lett.* **85**, 4353 (2000).
- ¹¹L. M. Helme *et al.*, *Physica B* **350**, 273(E) (2004).
- ¹²M. Sánchez-Andújar and Señarís-Rodríguez, *Solid State Sci.* **6**, 21 (2004).
- ¹³M. Sánchez-Andújar, B. Rivas-Murias, D. Rinaldi, R. Caciuffo, J. Mira, J. Rivas, and M. A. Señarís-Rodríguez, *J. Magn. Magn. Mater.* **272–276**, 855 (2004).
- ¹⁴Y. Shimada, S. Miyasaka, R. Kumai, and Y. Tokura, *Phys. Rev. B* **73**, 134424 (2006).
- ¹⁵S. Castro-García, M. Sánchez-Andújar, C. Rey-Cabezudo, M. A. Señarís-Rodríguez, and C. Julien, *J. Alloys Compd.* **323–324**, 710 (2001).
- ¹⁶K. Knížek, Z. Jiráček, J. Hejtmánek, M. Veverka, M. Maryško, G. Maris, and T. T. M. Palstra, *Eur. Phys. J. B* **47**, 213 (2005).
- ¹⁷A. J. Bray, *Phys. Rev. Lett.* **59**, 586 (1987).
- ¹⁸J. Wu and C. Leighton, *Phys. Rev. B* **67**, 174408 (2003).
- ¹⁹F. Fauth, E. Suard, and V. Caignaert, *Phys. Rev. B* **65**, 060401(R) (2001).
- ²⁰R. R. Gupta, *Landolt-Börnstein, New Series II/16* (Springer, Berlin, Heidelberg, 1986), p. 402.
- ²¹C. Autret, J. Hejtmánek, K. Knížek, M. Maryško, Z. Jiráček, M. Dlouhá, and S. Vratislav, *J. Phys.: Condens. Matter* **17**, 1601 (2005).
- ²²W. A. Harrison, in *The Electronic Structure and Properties of Solids* (Freeman, San Francisco, 1980).
- ²³X. L. Wang and E. Takayama-Muromachi, *Phys. Rev. B* **72**, 064401 (2005).
- ²⁴K. Knížek, Z. Jiráček, J. Hejtmánek, and P. Novák, *J. Phys.: Condens. Matter* **18**, 3285 (2006).
- ²⁵H. Watanabe, Y. Yamaguchi, H. Oda, and H. Takei, *J. Magn. Magn. Mater.* **15–18**, 521 (1980).